https://doi.org/10.5194/bg-2023-106
Preprint. Discussion started: 25 January 2024

Biogeosciences Discussions
Open Access
EGU

Predicting dominant terrestrial biomes at a global scale using machine learning algorithms, climate variable indices, and extreme climate indices

Hisashi SATO[1, 2]

[1] Research Institute for Global Change, Japan Agency for Marine-Earth Science and Technology (JAMSTEC), Yokohama, 236-0001, Japan
[2] Department of Ecosystem Studies, Graduate School of Agricultural and Life Sciences, The University of Tokyo, Tokyo, 113-8657, Japan

Correspondence to: Hisashi SATO (hsatoscb@gmail.com)

Abstract. Several methods have been proposed for modelling global biome distribution. Climate data are typically summarised in terms of a few climate indices. However, with the recent advancement of machine learning algorithms, such summarisation is no longer required. Extreme climate events such as intense droughts and very low temperatures cannot be captured by monthly mean climate data, which may limit the applicability of biome boundaries. In this study, I assessed the influences of machine learning algorithms, climate variable indices, and extreme climate indices on the accuracy and robustness of global biome modelling. I found that the random forest and convolutional neural network algorithms produced highly accurate models for reconstructing the global biome distribution. However, the convolutional neural network algorithm was preferable, because the random forest algorithm substantially overfit the training data relative to the other machine learning algorithms examined. Including indexed climate data slightly reduced model accuracy, whereas including extreme climate data slightly improved it. However, there were significant deviations in the distribution of values between the observed and predicted climate when extreme climate data was included; this fatally reduced the robustness of the models, which were evaluated in terms of prediction consistency. Therefore, I recommend that extreme climate data not be considered in global-scale biome prediction applications.

https://doi.org/10.5194/bg-2023-106
Preprint. Discussion started: 25 January 2024

1. Introduction

A biome is a major regional ecological community characterised by distinctive life forms and principal plant species (Lincoln et al., 1998). Biome distributions are useful for estimating land potential and raising public awareness about land change (reviewed in Hengl et al. (2018)). At the global scale, climate conditions largely determine biome distribution (Adams, 2010; Prentice et al., 1992), and biome distribution interacts with climate through biophysical and biochemical pathways (Pitman, 2003). Thus, biome distributions may also be applied in climate projection.

To date, several methods have been proposed for modelling biome distribution (Sato and Ise, 2022). In these models, climate data like monthly mean temperature and monthly precipitation are typically summarised as smaller numbers of climate indices such as annual precipitation and coldest month mean temperature. However, with the recent advancement of machine learning algorithms such as random forest (RF), restrictions on the amount of data used in model building have been relaxed, and it is no longer essential to summarise environmental data within indices. For example, Hengl et al. (2018) used 160 environmental variables including soil and topography, as well as non-indexed climate variables such as monthly precipitation and monthly average temperature to construct an empirical model of biome distribution using machine learning algorithms. However, increasing the number of variables in the model entails costs such as lower model adaptability and higher computational demand; therefore, it is still important to limit the number of variables included in the model.

From the perspective of plant physiology and ecology, the intensity of extreme climate events such as severe droughts and rare low-temperature incidents is a significant factor limiting biome boundaries (reviewed in Beigaite et al., 2022). Including extreme climate indices in addition to non-extreme climate variables has been reported to increase the accuracy of decision tree models (Beigaite et al., 2022).

In this study, I evaluated the accuracy of four machine learning algorithms in a global biome distribution model based on current climate characteristics. I also assessed the influence of including extreme climate indices or converting monthly precipitation and average air temperature (24 variables) into 16 climatic indices on model accuracy. To

https://doi.org/10.5194/bg-2023-106
Preprint. Discussion started: 25 January 2024

explore how the resulting models responded to climatic conditions beyond the training data, I applied them to forecast biome distributions for future climatic conditions (2060–2080) and compared their outputs.

2. Methods

2.1 Biome data

I used potential natural vegetation (PNV) compiled by Beigaite et al. (2022) to develop decision tree-based models of global PNV distribution (https://github.com/ritabei/dominant-natural-vegetation, accessed 20 June, 2022). The original PNV data were obtained from the Moderate Resolution Imaging Spectroradiometer (MODIS) MCD12C1 land cover product in 2001 (https://doi.org/10.5067/MODIS/MCD12C1.006). The MCD12C product contains three land cover classifications, among which Beigaite et al. (2022) used the International Geosphere Biosphere Programme (IGBP) land cover classification, which is primarily based on supervised learning classification of MODIS Terra and Aqua reflectance data (Friedl et al., 2010). The MCD12C1 product contains percent cover for 17 IGBP classes (Loveland and Belward, 1997) in each grid cell at a resolution of 0.05°. Beigaite et al. (2022) resampled the MCD12C1 data to 50 km × 50 km grids and extracted the dominant natural vegetation with the highest fraction in each grid cell. Among the original 17 categories, only 13 (natural vegetation) were used in this study (Figure 1, Table SI 1). Thus, grid cells with 100% human activity or water cover, or a combination of both, were eliminated from the analysis. I also ignored the continent of Antarctica. Ultimately, 52,297 grid cells were included in the analysis.

2.2 Climate data

This study used four climate datasets: averaged monthly air temperature and precipitation (*Ave*, 24 variables), averaged monthly climate indices (*AveI*, 16 variables), climate extreme indices representing extreme conditions on a daily scale such as the maximum length of a dry spell (*CEI*, 27 variables), and a subset of *CEI* (CEI_{part}, 21 variables). The variables included in *AveI* and *CEI* are listed in Tables SI 2 and SI 3, respectively. Figures

SI 1–3 show the present (1970–2000) and future (2061–2080) distributions of *Ave*, *AveI*, and *CEI*, respectively. Among all climatic variables used in this study, only six variables in the *CEI* dataset (Tn10p, Tx10p, Tn90p, Tx90p, WSDI, and CSDI) had completely separate variable distributions between the present and future. Another indexed extreme climate dataset, CEI_{part}, was constructed by excluding these variables from the *CEI* dataset.

Ave data were obtained from the WorldClim 2.1 product (released January 2020; Fick and Hijmans (2017)), which represents average monthly air temperature and precipitation data for 1970–2000. The original WorldClim 2.1 product was downloaded (http://worldclim.org, accessed 01 July, 2022) at a spatial resolution of 10 min, and resampled to 50 km × 50 km grids using the nearest-neighbour method. *AveI* was released by Beigaite et al. (2022), summarising WorldClim 2.1 properties in terms of annual means (e.g., BIO1 and BIO12), seasonality (e.g., BIO4, BIO7, and BIO15), and limiting environmental factors to a monthly scale (e.g., BIO5, BIO6, and BIO14).

The *CEI* product was released by Beigaite et al. (2022) using the CLIMDEX climate extremes index (Sillmann, 2013 #3057@@author-year; https://climate-modelling.canada.ca/climatemodeldata/climdex/). CLIMDEX comprises four datasets that were derived from different reanalysis datasets. Among these, Beigaite et al. (2022) used a dataset calculated from the ERA-Interim reanalysis dataset, which accurately reproduces observed climate extremes (Donat et al., 2014). *CEI* data derived from the ERA-Interim reanalysis dataset covers 32 years (1979–2010). For each grid, multi-year *CEI* values were averaged; multi-year averages of extreme indices are commonly used to represent averaged extreme conditions in the past and future (Seneviratne and Hauser, 2020; Sillmann et al., 2013a). The original resolution of the *CEI* data was 1.5° × 1.5°; they were transformed onto 10 min × 10 min grids through conservative interpolation and then resampled to 50 km × 50 km grids using nearest-neighbour interpolation.

For future climate condition projections (2061–2080), I used BIOCLIM (http://www.worldclim.com/cmip5_10m) and extreme climate variables (Sillmann et al. (2013b); https://crd-data-donnees-rdc.ec.gc.ca/CCCMA/products/CLIMDEX/CMIP5/) derived from future climate projections of the International Panel on Climate Change

https://doi.org/10.5194/bg-2023-106
Preprint. Discussion started: 25 January 2024

(IPCC) Coupled Model Intercomparison Project Phase 5 (CMIP5). I used only one future scenario, Representative Concentration Pathway (RCP) 8.5. In this study, RCPs represent atmospheric greenhouse gas (GHG) concentration forecasts adopted by the IPCC for its Fifth Assessment Report (AR5) in 2014; RCP8.5 assumes that global annual GHG emissions will continue to rise throughout the 21st century, resulting in 758 ppm of atmospheric CO_2 by 2080 (IPCC, 2013). All data were based on ensemble means of 11 models participating in CMIP5 and averaged over 2061–2080.

2.3 Machine learning algorithms

I employed four machine learning algorithms: RF (Breiman, 2001), support vector machine (SVM) (Cortes and Vapnik, 1995), naive Bayes classifier (NV) (Langley et al., 1992), and LeNet convolutional neural network (CNN). RF, SVM, and NV algorithms are commonly used to develop supervised learning models for classification. I implemented and evaluated these algorithms using the *randomForest*, *ksvm*, and *naiveBayes* packages in R v3.3.3 (R-Core-Team, 2018). I used the default model parameters for simplicity and to prevent potential overfitting, i.e., training the model too closely to a particular dataset, thereby creating a model that might fail to fit additional data or reliably predict future observations.

CNN algorithms are more complex than the others included in this study. They are typically applied to analyse visual imagery, and have been successfully adapted for species distribution modelling at regional (Benkendorf and Hawkins, 2020; Botella et al., 2018) and global scales (Sato and Ise, 2022). I follow Sato and Ise (2022) in training our CNN with graphical images as input variables representing climatic conditions.

In contrast to Beigaite et al. (2022), I did not include a decision tree algorithm in our study. Although decision trees rapidly provide interpretable boundary conditions for the distribution of a given output variable, they are generally inferior to the algorithms explored in this study in terms of reconstruction accuracy. The RF algorithm is an ensemble of decision tree algorithms, which I anticipated would provide higher model accuracy.

https://doi.org/10.5194/bg-2023-106
Preprint. Discussion started: 25 January 2024

2.4 Data analysis

To separate the influences of climate data and extreme climate indices on PNV model performance, I compared the learning performance of six climate dataset combinations: *Ave*, *Ave + CEI*, *Ave + CEI$_{part}$*, *AveI*, *AveI + CEI*, and *AveI + CEI$_{part}$*. Four machine learning algorithms were applied for each climate dataset combination, resulting in 24 models.

For each model, 25% of all 52,297 grids were randomly selected and used for training. I determined the test accuracy of each model by calculating the ratio of correct answers when the model was applied to the remaining 75% of grids. I also determined the training accuracy of each model by calculating the ratio of correct answers when the model was applied to the training data itself. Generally, training accuracy scores were expected to be higher than test accuracy scores due to overfitting (Leinweber, 2007); thus, an overfitting score was calculated as training accuracy minus test accuracy. Ten experiments were conducted for each model, and their averages were compared among models.

3. Results

Irrespective of the training datasets, all models except NV reconstructed global PNV precisely (Figs. 1 and SI4–7). The ranges of test accuracy values were 80.1%–81.4%, 74.6%–78.0%, 44.2%–50.1%, and 77.1%–82.0% for the RF, SVM, NV, and CNN models, respectively (Table 1). All accuracy values were > 17.8%, in which all grids were assumed to be the most frequent PNV, grassland (Table SI1). All accuracy values except for NV were > 49%, in which all grids at the same latitude were assigned the most frequent PNV at that latitude.

The low test accuracy of the NV model was caused by an overestimation of areas dominated by boreal forest, tropical rainforest, and deciduous broadleaf forest (Fig. 4), whereas the other models tended to show grid discrepancies along PNV boundaries (Figs. 2, 3, and 5). This trend corresponds to that of observation-based biome distributions being fragmented along PNV boundaries (Fig. 1). In contrast, model-reconstructed biome distributions have more continuous structures (Figs. SI4–7). From further analysis and discussion, I excluded the NV model due to its poor performance.

https://doi.org/10.5194/bg-2023-106
Preprint. Discussion started: 25 January 2024

The models shared common test accuracy patterns in response to input data (Table 1). The summarizing climate data into indices decreased model test accuracy, with *AveI* – *Ave* accuracy results of −1.1%, −1.8%, and −2.0% for RF, SVM, and CNN, respectively. The inclusion of extreme climate indices (*CEI*) increased test accuracy, with (*Ave* + *CEI*) − *Ave* accuracy results of 0.2%, 1.6%, and 1.0% for RF, SVM, and CNN, respectively, and (*AveI* + *CEI*) − *AveI* accuracy results of 1.1%, 3.1%, and 2.8% for RF, SVM, and CNN, respectively. Replacing *CEI* with CEI_{part} in these comparisons revealed no consistent trend in test accuracy, with negligible change for RF (0.1% vs. 0.1%), a decrease for SVM (−0.3% vs. −0.8%), and an increase for CNN (1.7% vs. 2.1%).

Training accuracy rates consistently exceeded test accuracy rates for all combinations of models and datasets (Tables 1 and 2), resulting in a positive overfitting score, defined as training accuracy minus test accuracy (Table 3). The RF model always had 100% training accuracy, resulting in high overfitting scores of 18.6%–20.0%. The overfitting scores of the other models were much lower, at 1.38%–2.05% for SVM and 0.75%–2.17% for CNN.

All models reconstructed highly coincident PNV distributions under current climatic conditions, irrespective of the training datasets (accuracy, 70.1%–86.4%, Table 4). For any combinations of models, datasets provide only slight differences in the correspondence of PNV reconstructions: in comparing RF and SVM, which provides the closest PNV distributions (accuracy, 84.5%–86.4%), the difference is less than 2.0%, while in comparing SVM and CNN, which provides the farthest PNV distributions (accuracy, 70.1%–72.4%), the difference is less than 2.3%.

When the trained models were adapted for a future climate, i.e., climate conditions beyond the training data, there were much larger differences between PNV distributions produced by different combinations of models and datasets (accuracy, 4.1%–82.8%, Table 5), with larger discrepancies in PNV maps constructed by models trained with *CEI* datasets (Figs. 6–9). SVM models trained with the *CEI* dataset output only evergreen broadleaf forest (Fig. SI9c, d), whereas CNN models output maps with abundant grassland and savanna (Fig. SI11c, d). Replacing *CEI* data with CEI_{part} data amended these extreme outputs (Figs. SI9e, f and 11e, f). Excluding models trained with the NV

https://doi.org/10.5194/bg-2023-106
Preprint. Discussion started: 25 January 2024

algorithm and *CEI* dataset produced highly coincident PNV distributions under a future climate (accuracy, 51.7%–82.8%, Table 5).

4. Discussion

Irrespective of the input dataset combination, the RF and CNN algorithms provided more accurate global PNV models than did the SVM and NV algorithms. Hengl et al. (2018) also found that RF consistently outperformed other machine learning algorithms, including neural networks. In their study, a stack of 160 global maps representing biophysical conditions over the terrestrial surface, including atmospheric, climatic, relief, and lithologic variables, were used as explanatory variables to predict 20 biome classes in the BIOME 6000 dataset (http://doi.org/10.17864/1947.99). Although a direct comparison with the findings of the current study is impossible, this previous report supports RF as a robust machine learning algorithm for reconstructing biome maps. The present study is the first to compare the results of a CNN algorithm adapted for biome modelling (Sato and Ise, 2022) to those of biome models based on other machine learning algorithms; this CNN showed comparable performance to an RF.

I found that RF and CNN algorithms had similar test accuracy rates. However, the CNN is preferable because RF produced much higher overfitting scores than any other machine learning algorithm examined in this study. Overfitting is an inevitable risk associated with empirical models (Leinweber, 2007). Fourcade et al. (2018) demonstrated an extreme example of pseudo-predicting variables (randomly chosen classical paintings) increasing the accuracy of species distribution modelling; these models sometimes had even higher evaluation scores than models trained with relevant environmental variables. To avoid overfitting or employing pseudo-predicting variables, Fourcade et al. (2018) suggested expending more effort in cross-validation and ensuring the selection of the most important predictors. I followed this suggestion in our analysis.

The climate index data used in this study reduced the number of variables by two thirds (from 24 to 16). However, it reduced model accuracy only slightly (−1.1%, −1.8%, and −2.0% for RF, SVM, and CNN, respectively), demonstrating that the typical climate indices used in this study adequately extracted essential climate information relevant to

https://doi.org/10.5194/bg-2023-106
Preprint. Discussion started: 25 January 2024

global biome distribution. Nevertheless, indexing has no particular merit in building machine learning-based invisible models, whereas it is essential in building visible models such as decision trees (Beigaite et al., 2022).

Adding extreme climate data improved test accuracy rates slightly but it can fatally reduce model robustness, which was defined as the consistency of model prediction under forecast climate conditions. This outcome was caused by six *CEI* variables with distributions that were entirely distinct from the training data, demonstrating the need to assess the distributions of training and predicting variables when building empirical models. Because the slight improvement in test accuracy obtained by including extreme climate data was insufficient to compensate the loss of model robustness, I recommend that extreme climate data not be included in models predicting global biome distribution at the geographical resolution employed in this study (0.5°).

There is clear evidence that climate extremes control plant demographic processes such as growth (Jolly et al., 2005; Ciais et al., 2005), regeneration (Ibanez et al., 2007), and mortality (Villalba and Veblen, 1998; Bigler et al., 2006), all of which influence plant species distributions. However, it does not follow that extreme climate data should always be considered to improve biome map reconstruction, because mean climatic values are tightly correlated with extreme climatic variables. Even indexed climate variables adequately extracted this correlated information in the present study, as shown by the slight differences in test accuracy rates between *Ave* and *AveI* (< 1.8%), and between *Ave* + CEI_{part} and *AveI* + CEI_{part} (< 0.8%), except for NV models (Table 1). However, at local and species levels, extreme climate may be a more critical predictor; Zimmermann et al. (2009) revealed that complementing mean climate predictors with variables representing climate extremes improves the predictive power of species distribution models.

A crucial disadvantage of the climatic envelope approach is that extrapolating current correlations between climate and biome distributions into the future may lead to seriously biased predictions. Thus, strong model performance under the present climate does not guarantee similar performance under a new set of climatic conditions that may occur in the future. However, no models except those trained with the NV algorithm and the *CEI* dataset showed apparent expansions of PNV uncertainty under projected climatic

https://doi.org/10.5194/bg-2023-106
Preprint. Discussion started: 25 January 2024

conditions. This result suggests that robust models can be developed beyond the training data if the machine learning algorithms and climatic variables are carefully selected. The climatic envelope approach has other limitations and disadvantages. For example, it ignores time lags between climate change and vegetation change, changes in atmospheric CO_2, and human land use change (discussed in Sato and Ise (2022)). However, the climatic envelope is helpful for various adaptations, including benchmarking dynamic global vegetation models (Fisher et al., 2018).

5. Conclusion

Models constructed based on RF and CNN algorithms provided accurate, robust global PNV models. Despite its slightly higher accuracy, the RF model tended to overfit the training data, leading to dramatically lower robustness; thus, the CNN model is preferable. The inclusion of climate data indices has no particular merit in developing "non-transparent" models, and only slightly reduced model accuracy. Extreme climate data improves model accuracy and robustness only if the distributions of climate variables are moderately within the range of the training data. Therefore, it is safer not to include extreme climate indices.

Data availability

All data required to reproduce the analyses described herein are publicly available at the following URL/DOI: https://doi.org/10.5281/zenodo.8113935.

Acknowledgements

This work was funded by the Arctic Challenge for Sustainability II (ArCS II) [Program Grant Number JPMXD1420318865]. The authors declare no conflicts of interest.

References

Adams, J.: Plants on the move, in: Vegetation-Climate Interaction - How Plants Make the Global Environment -, Second Edition ed., Springer, 67-96, 2010.
Beigaite, R., Tang, H., Bryn, A., Skarpaas, O., Stordal, F., Bjerke, J. W., and Zliobaite,

I.: Identifying climate thresholds for dominant natural vegetation types at the global scale using machine learning: Average climate versus extremes, Glob Chang Biol, 28, 3557-3579, 10.1111/gcb.16110, 2022.

Benkendorf, D. J. and Hawkins, C. P.: Effects of sample size and network depth on a deep learning approach to species distribution modeling, Ecological Informatics, 60, 10.1016/j.ecoinf.2020.101137, 2020.

Bigler, C., Bräker, O. U., Bugmann, H., Dobbertin, M., and Rigling, A.: Drought as an Inciting Mortality Factor in Scots Pine Stands of the Valais, Switzerland, Ecosystems, 9, 330-343, 10.1007/s10021-005-0126-2, 2006.

Botella, C., Joly, A., Bonnet, P., Monestiez, P., and Munoz, F.: A Deep Learning Approach to Species Distribution Modelling, in: Multimedia Tools and Applications for Environmental & Biodiversity Informatics, edited by: Joly, A., Vrochidis, S., Karatzas, K., Karppinen, A., and Bonnet, P., Springer Nature, 169-199, 10.1007/978-3-319-76445-0_10, 2018.

Breiman, L.: Random Forests, Machine Learning, 45, 5-32, 10.1023/a:1010933404324, 2001.

Ciais, P., Reichstein, M., Viovy, N., Granier, A., Ogee, J., Allard, V., Aubinet, M., Buchmann, N., Bernhofer, C., Carrara, A., Chevallier, F., De Noblet, N., Friend, A. D., Friedlingstein, P., Grunwald, T., Heinesch, B., Keronen, P., Knohl, A., Krinner, G., Loustau, D., Manca, G., Matteucci, G., Miglietta, F., Ourcival, J. M., Papale, D., Pilegaard, K., Rambal, S., Seufert, G., Soussana, J. F., Sanz, M. J., Schulze, E. D., Vesala, T., and Valentini, R.: Europe-wide reduction in primary productivity caused by the heat and drought in 2003, Nature, 437, 529-533, 10.1038/nature03972, 2005.

Cortes, C. and Vapnik, V.: Support-vector networks, Machine Learning, 20, 273-297, 10.1007/bf00994018, 1995.

Donat, M. G., Sillmann, J., Wild, S., Alexander, L. V., Lippmann, T., and Zwiers, F. W.: Consistency of Temperature and Precipitation Extremes across Various Global Gridded In Situ and Reanalysis Datasets, J. Clim., 27, 5019-5035, 10.1175/jcli-d-13-00405.1, 2014.

Fick, S. E. and Hijmans, R. J.: WorldClim 2: new 1-km spatial resolution climate surfaces for global land areas, Int. J. Climatol., 37, 4302-4315, 10.1002/joc.5086, 2017.

Fisher, R. A., Koven, C. D., Anderegg, W. R. L., Christoffersen, B. O., Dietze, M. C., Farrior, C. E., Holm, J. A., Hurtt, G. C., Knox, R. G., Lawrence, P. J., Lichstein, J. W., Longo, M., Matheny, A. M., Medvigy, D., Muller-Landau, H. C., Powell, T. L., Serbin, S. P., Sato, H., Shuman, J. K., Smith, B., Trugman, A. T., Viskari, T., Verbeeck, H., Weng, E., Xu, C., Xu, X., Zhang, T., and Moorcroft, P. R.: Vegetation demographics in Earth System Models: A review of progress and priorities, Glob Chang Biol, 24, 35-54, 10.1111/gcb.13910, 2018.

Fourcade, Y., Besnard, A. G., and Secondi, J.: Paintings predict the distribution of species, or the challenge of selecting environmental predictors and evaluation statistics, Global Ecol. Biogeogr., 27, 245-256, 10.1111/geb.12684, 2018.

Friedl, M. A., Sulla-Menashe, D., Tan, B., Schneider, A., Ramankutty, N., Sibley, A., and Huang, X.: MODIS Collection 5 global land cover: Algorithm refinements and characterization of new datasets, Remote Sens. Environ., 114, 168-182, 10.1016/j.rse.2009.08.016, 2010.

Hengl, T., Walsh, M. G., Sanderman, J., Wheeler, I., Harrison, S. P., and Prentice, I. C.: Global mapping of potential natural vegetation: an assessment of machine learning algorithms for estimating land potential, Peerj, 6, 10.7717/peerj.5457, 2018.
Ibanez, I., Clark, J. S., LaDeau, S., and HilleRisLambers, J.: Exploiting temporal variability to understand tree recruitment response to climate change, Ecol. Monogr., 77, 163-177, 10.1890/06-1097, 2007.
IPCC: Climate change 2013: The physical science basis. Contribution of Working Group I to the fifth assessment report of the Intergovernmental Panel on Climate Change, Cambridge, United Kingdom and New York, NY, USA2013.
Jolly, W. M., Dobbertin, M., Zimmermann, N. E., and Reichstein, M.: Divergent vegetation growth responses to the 2003 heat wave in the Swiss Alps, Geophys. Res. Lett., 32, n/a-n/a, 10.1029/2005gl023252, 2005.
Langley, P., Iba, W., and Thompson, K.: An analysis of Bayesian classifiers, Tenth NationalConference on Artificial Intelligence, Menlo Park, CA, 223–228,
Leinweber, D. J.: Stupid data miner tricks: Overfitting the S&P 500, The Journal of Investing, 16, 15-22, https://doi.org/10.3905/joi.2007.681820, 2007.
Lincoln, R., Boxshall, G., and Clark, P.: A Dictionary of Ecology, Evolution and Systematics, 2nd edition, University Press, Cambridge, United Kingdom 1998.
Loveland, T. R. and Belward, A. S.: The International Geosphere Biosphere Programme Data and Information System global land cover data set (DISCover), Acta Astronaut., 41, 681-689, 10.1016/s0094-5765(98)00050-2, 1997.
Pitman, A. J.: The evolution of, and revolution in, land surface schemes designed for climate models, Int. J. Climatol., 23, 479-510, 2003.
Prentice, I. C., Cramer, W., Harrison, S. P., Leemans, R., Monserud, R. A., and Solomon, A. M.: A global biome model based on plant physiology and dominance, soil properties and climate, J. Biogeogr., 19, 117-134, doi.org/10.2307/2845499, 1992.
R-Core-Team: R: A Language and Environment for Statistical Computing, R Foundation for Statistical Computing [code], 2018.
Sato, H. and Ise, T.: Predicting global terrestrial biomes with the LeNet convolutional neural network, Geoscientific Model Development, 15, 3121-3132, 10.5194/gmd-15-3121-2022, 2022.
Seneviratne, S. I. and Hauser, M.: Regional Climate Sensitivity of Climate Extremes in CMIP6 Versus CMIP5 Multimodel Ensembles, Earths Future, 8, e2019EF001474, 10.1029/2019EF001474, 2020.
Sillmann, J., Kharin, V. V., Zhang, X., Zwiers, F. W., and Bronaugh, D.: Climate extremes indices in the CMIP5 multimodel ensemble: Part 1. Model evaluation in the present climate, Journal of Geophysical Research: Atmospheres, 118, 1716-1733, 10.1002/jgrd.50203, 2013a.
Sillmann, J., Kharin, V. V., Zwiers, F. W., Zhang, X., and Bronaugh, D.: Climate extremes indices in the CMIP5 multimodel ensemble: Part 2. Future climate projections, Journal of Geophysical Research: Atmospheres, 118, 2473-2493, 10.1002/jgrd.50188, 2013b.
Villalba, R. and Veblen, T. T.: Influences of Large-Scale Climatic Variability on Episodic Tree Mortality in Northern Patagonia, Ecology, 79, 2624-2640, 10.1890/0012-9658(1998)079[2624:Iolscv]2.0.Co;2, 1998.

https://doi.org/10.5194/bg-2023-106
Preprint. Discussion started: 25 January 2024

Zimmermann, N. E., Yoccoz, N. G., Edwards, T. C., Meier, E. S., Thuiller, W., Guisan, A., Schmatz, D. R., and Pearman, P. B.: Climatic extremes improve predictions of spatial patterns of tree species, Proceedings of the National Academy of Sciences of the United States of America, 106, 19723-19728, 10.1073/pnas.0901643106, 2009.

https://doi.org/10.5194/bg-2023-106
Preprint. Discussion started: 25 January 2024

Biogeosciences
Discussions

Tables

Table 1. Average test accuracy rates ± standard deviation (%; n = 10) for models based on four machine learning algorithms: random forest (RF), support vector machine (SVM), Naive Bayes classifier (NV), and convolutional neural network (CNN). Input variable abbreviations: *Ave*, averaged monthly air temperature and precipitation; *AveI*, averaged monthly climate indices; *CEI*, climate extreme indices; and CEI_{part}, a subset of *CEI*.

Input variable combinations	RF	SVM	NV	CNN
Ave	81.2 ± 0.21	76.4 ± 0.15	46.7 ± 0.84	79.1 ± 0.15
Ave + CEI	81.4 ± 0.20	78.0 ± 0.15	45.2 ± 1.20	80.1 ± 0.12
$Ave + CEI_{part}$	81.5 ± 0.22	77.7 ± 0.19	44.2 ± 1.24	81.8 ± 0.30
AveI	80.1 ± 0.22	74.6 ± 0.12	50.1 ± 0.88	77.1 ± 0.18
AveI + CEI	81.2 ± 0.21	77.7 ± 0.19	44.6 ± 1.82	79.9 ± 0.16
$AveI + CEI_{part}$	81.3 ± 0.18	76.9 ± 0.16	43.3 ± 2.26	82.0 ± 0.31

https://doi.org/10.5194/bg-2023-106
Preprint. Discussion started: 25 January 2024

Table 2.

As in Table 1, but for training accuracy rate ± standard deviation (%, n = 10).

Input variable combinations	RF	SVM	NV	CNN
Ave	100.0 ± 0.00	77.8 ± 0.28	46.8 ± 0.70	81.1 ± 0.90
Ave + *CEI*	100.0 ± 0.00	79.9 ± 0.25	45.3 ± 1.02	81.9 ± 0.94
Ave + CEI_{part}	100.0 ± 0.00	79.5 ± 0.32	44.4 ± 1.08	83.0 ± 0.44
AveI	100.0 ± 0.00	76.1 ± 0.33	50.5 ± 0.97	78.3 ± 1.02
AveI + *CEI*	100.0 ± 0.00	79.8 ± 0.14	44.7 ± 1.74	82.1 ± 0.90
AveI + CEI_{part}	100.0 ± 0.00	78.5 ± 0.38	43.5 ± 2.14	82.9 ± 0.48

Table 3.

As in Table 1, but for overfitting scores ± standard deviation (%, n = 10).

	RF	SVM	NV	CNN
Ave	18.9 ± 0.21	1.38 ± 0.30	0.11 ± 0.40	2.05 ± 0.99
Ave + *CEI*	18.7 ± 0.20	1.92 ± 0.30	0.15 ± 0.36	1.78 ± 0.91
Ave + CEI_{part}	18.6 ± 0.22	1.83 ± 0.43	0.14 ± 0.32	0.75 ± 0.62
AveI	20.0 ± 0.22	1.53 ± 0.39	0.33 ± 0.59	1.19 ± 1.03
AveI + *CEI*	18.8 ± 0.21	2.05 ± 0.29	0.15 ± 0.49	2.17 ± 0.86
AveI + CEI_{part}	18.8 ± 0.18	1.91 ± 0.46	0.16 ± 0.43	1.06 ± 0.57

https://doi.org/10.5194/bg-2023-106
Preprint. Discussion started: 25 January 2024

Table 4. Degree of coincidence (%) in pairwise comparisons of simulated potential natural vegetation (PNV) under the current climate. Asterisks indicate the exclusion of models trained with the naive Bayes classifier.

	RF vs SVM	RF vs NV	RF vs CNN	SVM vs NV	SVM vs CNN	NV vs CNN
Ave	85.6*	49.4	70.8*	50.9	70.1*	33.5
Ave + CEI	86.4*	47.8	71.5*	49.0	72.3*	32.0
Ave + CEI_{part}	86.3*	46.1	74.1*	46.9	70.6*	30.4
AveI	84.4*	53.8	70.8*	56.7	71.9*	38.8
AveI + CEI	86.1*	46.9	70.9*	48.1	72.4*	31.2
AveI + CEI_{part}	85.5*	45.0	73.5*	46.0	70.7*	29.2

Table 5. Degree of coincidence (%) in pairwise comparisons of simulated potential natural vegetation (PNV) under a Representative Concentration Pathway 8.5 (RCP8.5) climate scenario. Asterisks indicate the exclusion of models trained with the naive Bayes classifier or including climate extreme indices as input data.

	RF vs SVM	RF vs NV	RF vs CNN	SVM vs NV	SVM vs CNN	NV vs CNN
Ave	78.6*	46.0	56.3*	52.8	65.4*	35.8
Ave + CEI	3.4	21.0	43.4	20.2	1.6	2.8
Ave + CEI_{part}	82.8*	45.7	63.1*	51.2	51.7*	30.6
AveI	81.2*	51.5	60.8*	56.9	65.4*	37.7
AveI + CEI	4.1	22.0	56.8	17.5	5.1	10.2
AveI + CEI_{part}	82.0*	44.9	66.3*	49.4	66.0*	30.0

https://doi.org/10.5194/bg-2023-106
Preprint. Discussion started: 25 January 2024

Figures

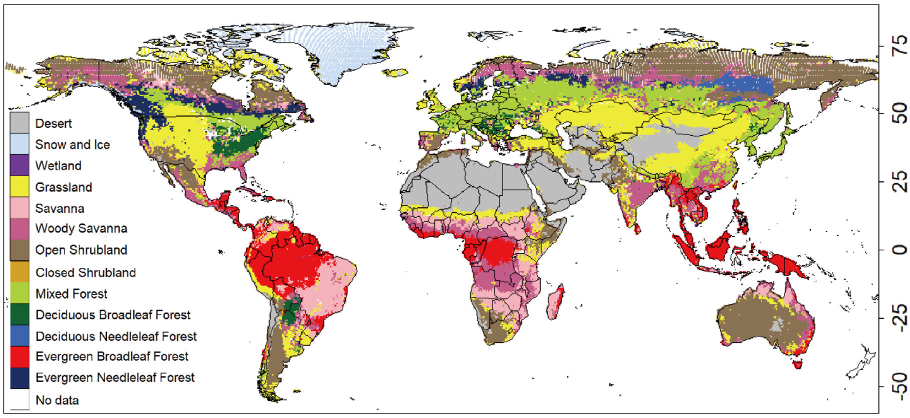

Figure 1

Distribution of observation-based potential natural vegetation (PNV) data, which were used to train machine learning-based models in this study.

https://doi.org/10.5194/bg-2023-106
Preprint. Discussion started: 25 January 2024

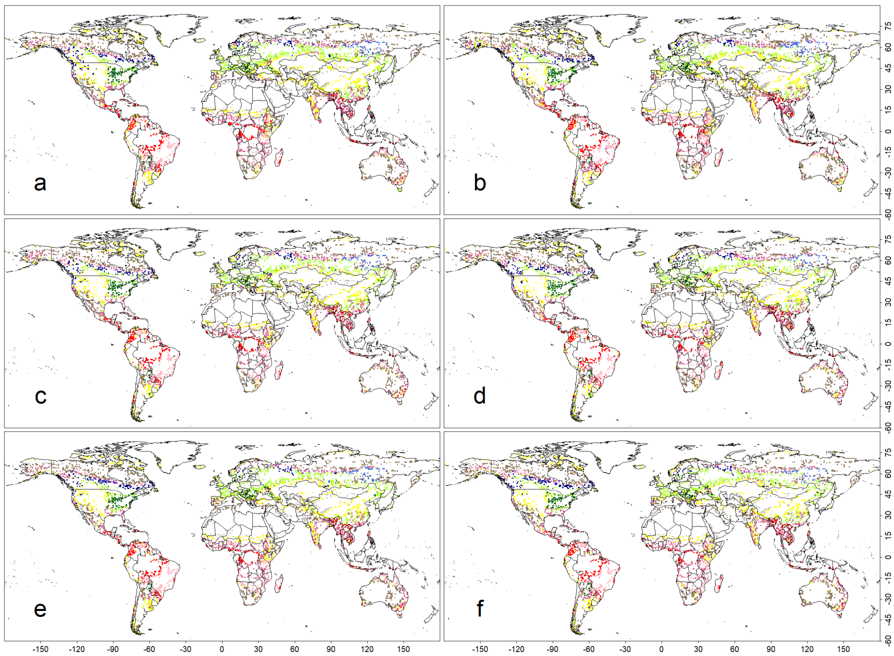

Figure 2. Differences in simulated PNV under the current climate between a random forest (RF) algorithm-based model and PNV observation data. Four sets of climate data were used for training and simulation: (a) averaged monthly air temperature and precipitation (*Ave*), (b) averaged monthly climate indices (*AveI*), (c) Ave + climate extreme indices (*CEI*), (d) *AveI* + *CEI*, (e) *Ave* + a subset of *CEI* (CEI_{part}), and (f) *AveI* + CEI_{part}. Color definitions are available in Fig. 1.

https://doi.org/10.5194/bg-2023-106
Preprint. Discussion started: 25 January 2024

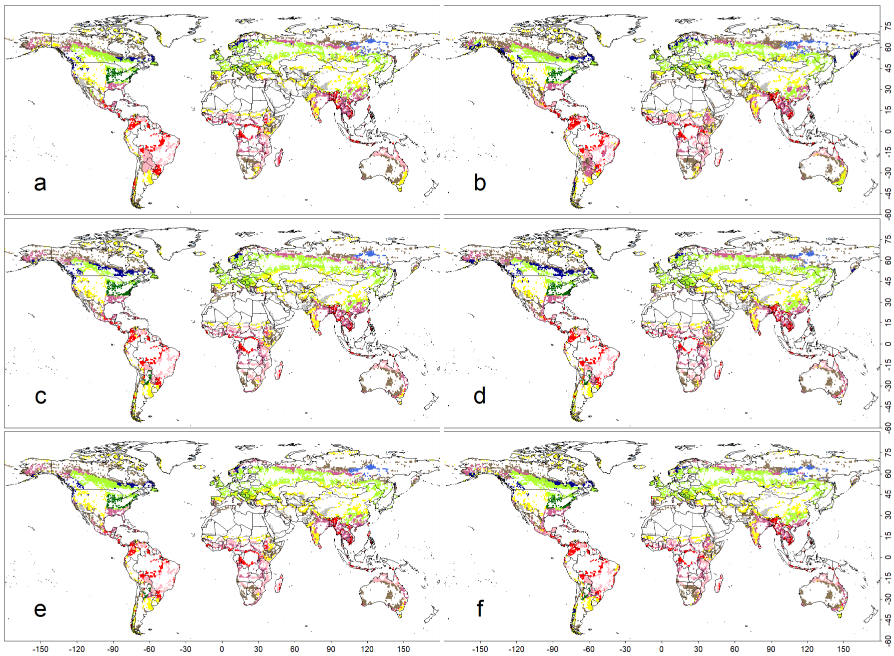

Figure 3. As in Fig.2, but for a support vector machine (SVM)-based model.

https://doi.org/10.5194/bg-2023-106
Preprint. Discussion started: 25 January 2024

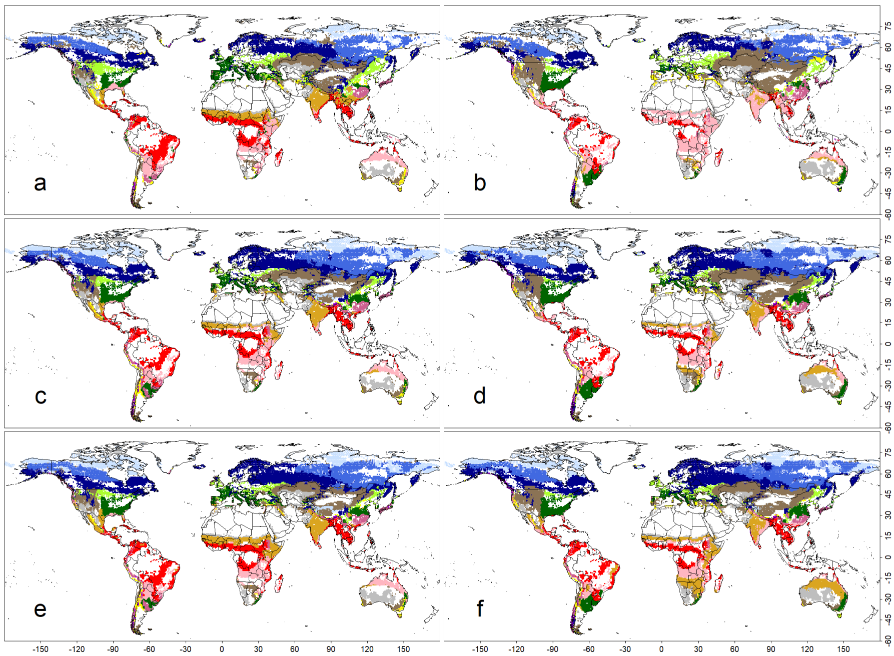

Figure 4. As in Fig. 2, but for a naive Bayes classifier (NV)-based model.

https://doi.org/10.5194/bg-2023-106
Preprint. Discussion started: 25 January 2024

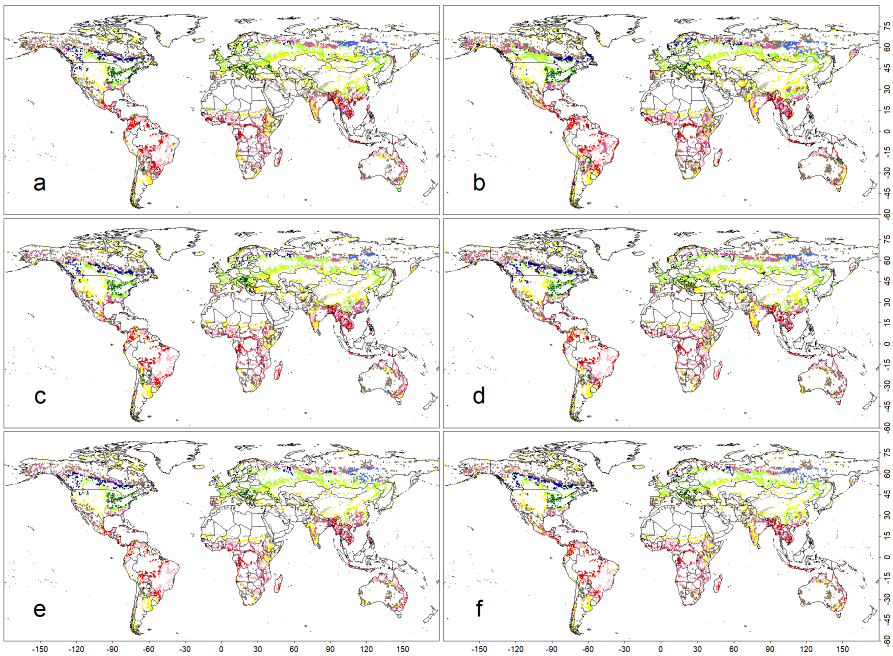

Figure 5. As in Fig. 2, but for a convolutional neural network (CNN)-based model.

https://doi.org/10.5194/bg-2023-106
Preprint. Discussion started: 25 January 2024

Biogeosciences
Discussions
Open Access

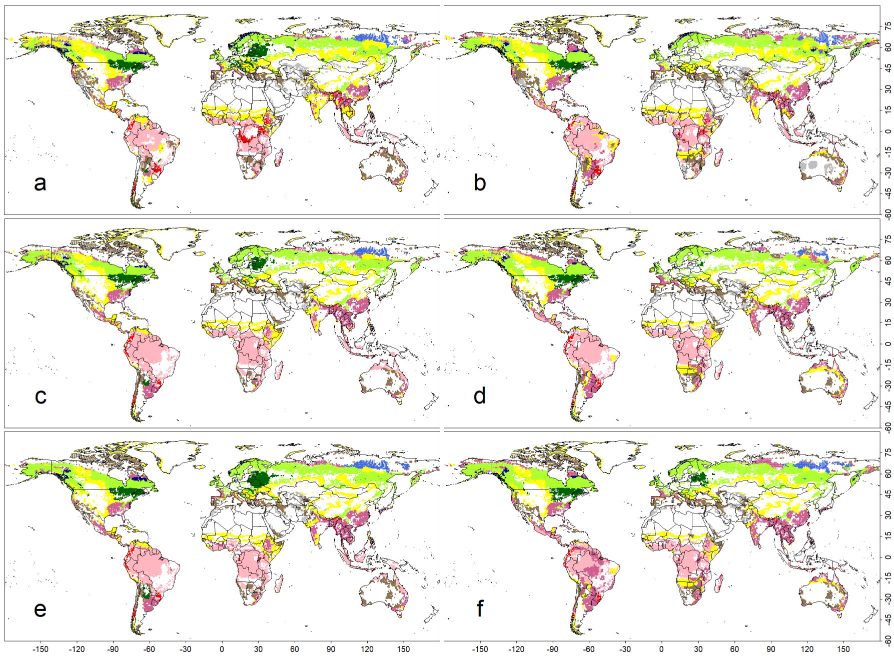

Figure 6. Differences in simulated PNV between the current climate and a Representative Concentration Pathway 8.5 (RCP8.5) climate scenario for 2080 produced by a random forest (RF)-based model. Four sets of climate data were used for training and simulation: (a) averaged monthly air temperature and precipitation (*Ave*), (b) averaged monthly climate indices (*AveI*), (c) *Ave* + climate extreme indices (*CEI*), (d) *AveI* + *CEI*, (e) *Ave* + a subset of *CEI* (CEI_{part}), and (f) *AveI* + CEI_{part}. Color definitions are available in Fig. 1.

https://doi.org/10.5194/bg-2023-106
Preprint. Discussion started: 25 January 2024

Biogeosciences
Discussions
Open Access

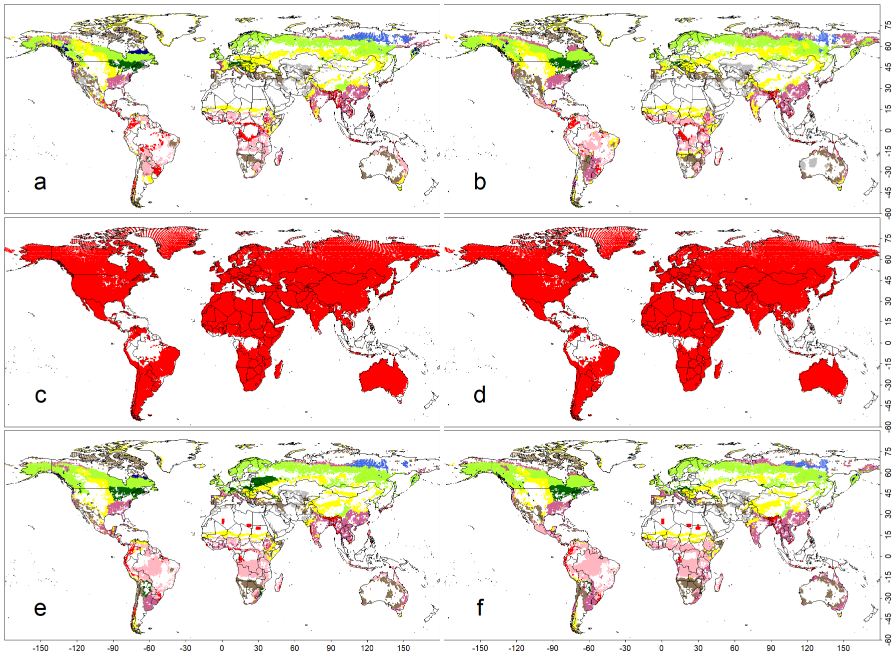

437

438 Figure 7. As in Fig.6, but for a support vector machine (SVM)-based model.

https://doi.org/10.5194/bg-2023-106
Preprint. Discussion started: 25 January 2024

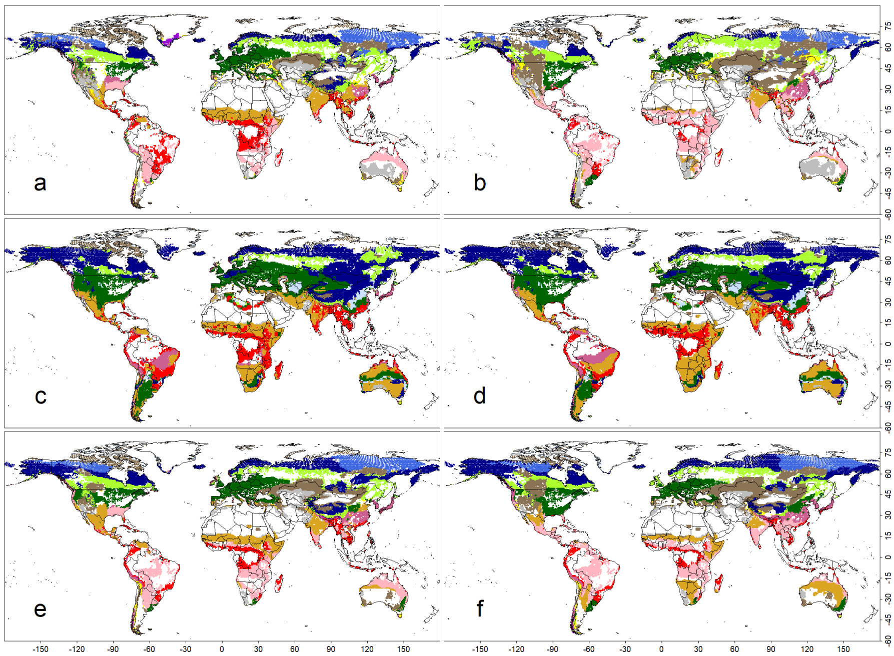

Figure 8. As in Fig.6 but for a naive Bayesian classifier (NV)-based model.

https://doi.org/10.5194/bg-2023-106
Preprint. Discussion started: 25 January 2024

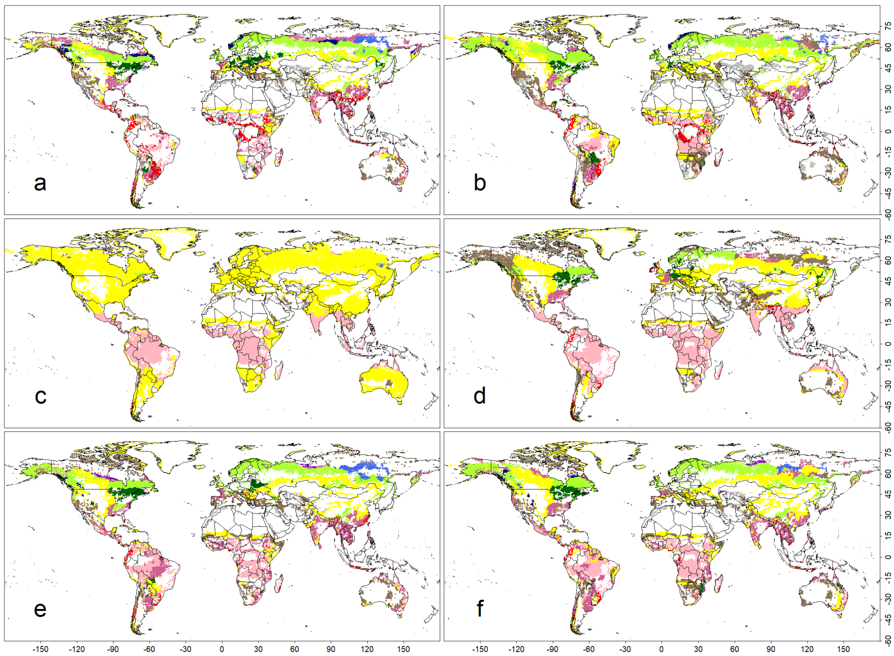

Figure 9. As in Fig.6, but for a convolutional neural network (CNN)-based model.